Proceedings of ASME Turbo Expo 2008: Power for Land, Sea and Air
GT2008
June 9-13, 2008, Berlin, Germany

GT2008-50958

COMBUSTION CHARACTERISTICS OF HYDROGEN-METHANE HYBRID FUELS IN COFLOW JET DIFFUSION FLAMES

Hui Wu，Wenxing Zhang
wuhui0443@sina.com.cn
Graduate University of Chinese Academy of Sciences
P. O. Box 2706, Beijing China, 100080

Kejin Mu, Yue Wang, and Yunhan Xiao
Advanced Energy and Power Technology Laboratory, Institute of Engineering Thermophysics (IET), Chinese Academy of Sciences.
P. O. Box 2706, Beijing China, 100080

ABSTRACT

As the development and increasingly widespread use of IGCC and zero emission energy system, the development of advanced combustion capabilities for gaseous hydrogen and hydrogen rich fuels in gas turbine applications is becoming an area of much great concern. The combustion characteristics of hydrogen rich fuel is very different from nature gas in aspects such as flame stability, flame temperature, combustor acoustics, pollutant emissions, combustor efficiency, and some other important quantities. However, few of these issues are clearly understood by far.

The purpose of this paper is to compare in detail the combustion performance of hydrogen-methane hybrid fuels with various volumetric H_2 fractions ranging from 0% to 100%. Meanwhile, the comparison of pure H_2, pure CH_4, and $80\%H_2+20\%CH_4$ was the emphasis. $80\%H_2+20\%CH_4$ hybrid gas is selected expressly because its component is approximately equal to the outcome of a hydrogen production test bed of our laboratory, and it is considered by the team to be a potential transition fuel of gas turbines between nature gas and pure hydrogen.

Detailed experimental measurements and numerical simulations were conducted using a coflow jet diffusion burner. It was found that in the extent of experiments, when under equal general power, the flame length of hydrogen contained fuels wasn't much shorter than methane, and didn't get shorter with the increase of H_2 fraction as expected. That was because the shortening tendency caused by the increase of H_2 fraction was counteracted partially by the increase of fuel velocity, results of which was the extending of flame length.

Maximum temperature of H_2 flame was 1733K, which was 30K higher than $80\%H_2+20\%CH_4$ and 120K higher than CH_4. All of the highest temperatures of the three fuels were presented at the recirculation zone of the flame. Although it seemed that the flame of CH_4 had the longest dimension compared with H_2 contained fuels when observed through photos, the high temperature region of flames was getting longer when increasing H_2 fractions. Curves of temperature distribution predicted by all the four combustion models in FLUENT investigated here had a departure away from the experimental data. Among the models, Flamelet model was the one whose prediction was comparatively close to the experimental results.

Flame of H_2 and $80\%H_2+20\%CH_4$ had a much better stability than flame of CH_4, they could reach a so called recirculating flame phase and never been blew out in the extent of experiments. On the contrary, CH_4 flames were blew out easily soon after they were lifted up.

Distribution of OH concentration at the root of flames showed that the flame boundary of H_2 and $80\%H_2+20\%CH_4$ was more clearly than CH_4. That is to say, at the root of the flame, combustion of H_2 was the most intensive one, $80\%H_2+20\%CH_4$ took the second place, while CH_4 was the least.

NOx emissions didn't show a linear relationship with the volumetric fraction of H_2, but showed an exponential uptrend instead. It presented a fairly consistent tendency with flame

temperature, which proved again there was a strong relationship between flame temperature and NOx emissions in the combustion of hydrogen contained fuels.

If adding CH_4 into pure H_2, NOx concentration would have a 17.2ppm reduction with the first 20% accession, but only 11.1ppm with the later 80% accession. Hence, if NOx emission was the only aspect to be considered, $80\%H_2+20\%CH_4$ seemed to be a better choice of transition fuel from pure CH_4 to pure H_2.

NOMENCLATURE

i	The number of moles of oxygen combining with one mole of combustible gas
k	Coefficient of interdiffusion
D	Diameter of fuel tubes
h	Axial distance away from fuel nozzle
*U*e	Mean axial annular air-flow velocity (m/s)
*U*j	Mean axial central fuel-jet velocity (m/s)

INTRODUCTION

For the reduction of pollutant emission in the process of energy utilization, especially for the realization of CO_2 zero emission, hydrogen is becoming more and more attractive as a potential alternative for fossil fuels. However, there might be many problems for traditional combustion equipments to use pure hydrogen straightly, since hydrogen has some characteristics that strongly deviate from the main components of conventional fuels, such as methane. On the other hand, there are some middle productions which contain not only hydrogen, but also hydrocarbons in the process of hydrogen production. For example, in our laboratory, a single-step hydrogen production equipment can produce a hybrid gas which contains about 80% hydrogen and 20% methane [1, 2]. These hydrogen-hydrocarbon hybrid gas might be a good transitional fuel between traditional fossil fuels and pure hydrogen. Therefore, research works should be conducted to find out their combustion characteristics. The object of this paper is to study the dissimilarities of hydrogen, methane, and hydrogen-methane hybrid fuels, especially 80% hydrogen plus 20%methane (in volumetric fraction).

Some researchers have done experiments or numerical simulations to study diffusion flames of hydrogen-hydrocarbon composite fuels [3-7]. In their papers, different fuels are usually compared in equal flow rate. In fact, hydrogen has much lower volumetric heat value than methane. Hence, to achieve equal power, more quantity of hydrogen should be combusted. Hence, comparison of the fuels in equal general power might be more significant.

The diffusion flame is the most common type of flame applied in practical combustion devices, and the coflow jet diffusion flame is a simple but effective model for study basic combustion characteristics of fuels. Therefore, it was selected as the first step of our research project. Swirl diffusion flames and premixed flames of the hydrogen-hydrocarbon hybrid fuels will be studied later, but not in this paper.

EXPEIMENTAL PROCEDURE

The experimental apparatus of this paper was a laboratory-scale coflow jet diffusion bluff-body burner, showed in fig 1 (dimensions are in millimeter). Fuel was injected from the central tube directly into quiescent atmosphere, and air was injected from the annular space around the fuel tube. The area of air jet channel was fixed, while dimension of the fuel tube could be changed. Three fuel tubes with diameter of 6mm, 9mm, and 11mm was used in the experiments.

The fuel tube was a little bit higher than the annular air injecting section, as shown in fig 1. Thus, a bluff-body was formed to stabilize the flame. A recirculation zone could be seen clearly during the experiments.

When NOx emissions was measured, a chimney with inner diameter of 110mm and height of 1200mm was fixed upon the burner, and a water-cooled sample probe entered into the chimney from sampling holes protruded from the chimney wall.

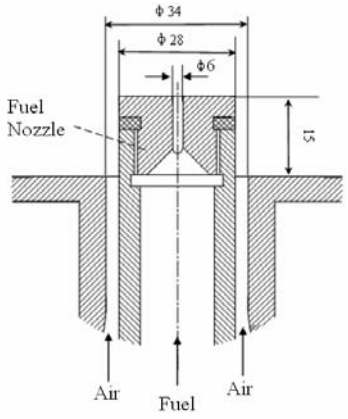

Fig.1 Structure of the Burner

Table 1 showed the parameters of fuels in the experiments. All of these fuels had equal general power of $2.675x10^7$J/h. The flow rate of the air was $7.2m^3$/h, corresponding velocity was 6.85m/s. The equivalent ratio was 0.99 for CH_4 and 0.83 for H_2, while ratios for other fuels were between 0.99 and 0.83. The velocity values in the table are under Φ=6mm fuel tube. Besides, for studying influences of tube dimension and fuel velocity on the flame structure, fuel tubes with diameter of 9mm and 11mm were used respectively for $80\%H_2+20\%CH_4$ and pure H_2, to keep equal fuel velocity with pure CH_4 (7.39m/s in ϕ6 tube). All experiments were done under normal pressure and room temperature.

Photos of flames were taken by a camera with exposure length of 4 seconds. Temperatures of flames were measured by a butt-weld thermocouple which was based on a design presented by Cundy et al [8]. The thermocouples employed in the experiments were uncoated type R (Pt-Pt/13%Rh) wire pairs. The conduction and radiation errors were corrected by a correctional calculation method applicable to gas bodies with steep gradients when a thermocouple of the larger diameter is used [9]. The following expression can be used to estimate the temperature

error band (e.g. 70K correction to the probe temperature in order to obtain a 1000K gas temperature):

$$\Delta T = T_g - T_p = \frac{1.25\varepsilon\sigma d^{0.75}}{k_g} \bullet \left(\frac{v}{u}\right)^{0.25} \bullet \left(T_p^4 - T_w^4\right)$$

NOx emissions were measured by a MRU VARIO Plus emission monitoring system, while flue gas was sampled by a water-cooled sample probe.

H_2 (volumetric fraction)	CH_4 (volumetric fraction)	flow rate (m^3/h)	velocity of flow (m/s)
100%	0%	2.50	24.57
90%	10%	2.03	19.95
80%	20%	1.71	16.80
70%	30%	1.47	14.45
60%	40%	1.29	12.68
50%	50%	1.15	11.3
40%	60%	1.04	10.23
30%	70%	0.95	9.32
20%	80%	0.87	8.55
10%	90%	0.81	7.92
0%	100%	0.75	7.39

Table.1 Parameters of fuels

OH concentrations were measured by a PLIF, principle of which was showed in figure 2.

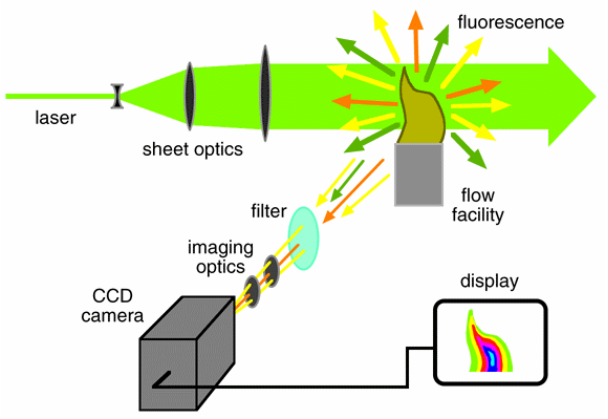

Fig.2 Sketch of PLIF System

As the figure showed, a bind of laser with wavelength of 355nm generated by a Nd:YAG laser (Spectra-physics) enters into a dye laser (Sirah), then generates a second laser of 567nm wavelength. The second laser passes through a BBO octave crystal and a spectroscope to generate a UV-light with wavelength of 283.55nm. After that, the UV-light passed through a series of sheet optics and becomes a sheet light with width of 120mm and thickness of 0.5mm. This sheet light is used to excitated the OH radicals in the flame to produce fluorescence. An ICCD (La Vision) with narrowband filter (BP308/10) is mounted on a befitting location to record the fluorescence.

NUMERICAL SIMULATION

FLUENT and CHEMKIN was used in this paper to predict flame temperature and the location of flame front.

In the simulation of FLUENT, the standard *k*-ε model was employed for turbulent flow. Four combustion models, Eddy-Dissipation and EDC under Species Transport Model, Non-Adiabatic Steady Flamelet and Equilibrium under Non-Premixed Combustion Model, were investigated through comparing temperature predicted results of them with the data of experiments. Results showed that Flamelet was the model who approached experimental results most. Therefore, Flamelet model was used finally for predicting the flame temperatures of various fuels. The reaction kinetics used in the Flamelet model was GRI3.0 mechanism, which including 53 species and 325 elementary reactions.

A well known opposed-flow flame model was used in CHEMKIN for research the orderliness of flame front changing along with the increase of hydrogen fraction in fuels. Opposed diffusion flame was often used to study basal characteristics of non-premixed flames. GRI3.0 mechanism was also used here. The velocity of fuel and air was both 100cm/s. Distance between the two circular nozzles was 2.0cm, fuel at axial distance of 0cm and air at distance of 2.0cm.

RESULTS AND ANALYSIS

Flame Structure

Photos of H_2, CH_4 and 80%H_2+20%CH_4 in ϕ6 fuel tube were shown in figure 3.

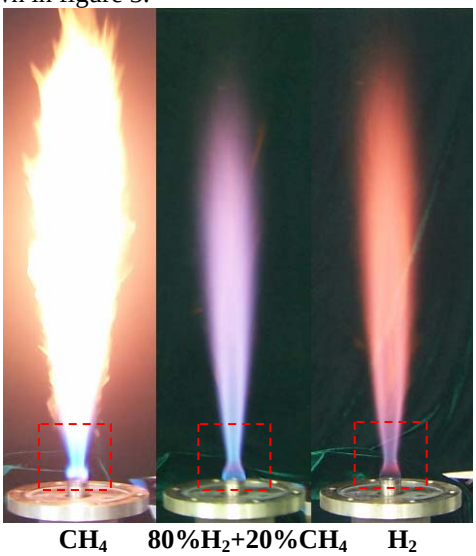

CH_4 80%H_2+20%CH_4 H_2

Fig.3 Photos of Flames in ϕ6 Fuel Tube

As the photos showed, flame of methane was more luminous than the two of others, flame of the 80%H_2+20%CH_4 was blue in color, while flame of pure hydrogen was in reddish glow. Although pure hydrogen should be invisible, the luminosity and colors observed here may be caused by the impurity of fuel or air.

The length of flames is an important parameter to be concerned, due to its significance in the designing of combustors. Many literatures figured out that the flame length would be shortened when adding hydrogen into hydrocarbon fuels. However, that happened only when the total flow rate was unchanged. As was mentioned above, for obtaining equal power, the volumetric flow rate of hydrogen contained fuels must be larger than methane. In this paper, the flow rate of pure hydrogen is about 2.3 times higher than that of pure methane. And flow rate of other fuels was increased along with the increase of H_2 fraction, as shown in table 1. Under this condition, we could see from figure 3 that the flame length of H_2 and 80%H_2+20%CH_4 was only a little bit shorter than that of CH_4. In fact, flame length of fuels with various H_2 fractions had little difference which was hardly visible in the experiments.

S.P Burke and T.E. Schumann had analyzed in detail all the factors that influence the flame length of coflow jet diffusion burner in their paper [10]. According to their analysis, these factors include dimensions of tubes, diffusion coefficient of fuels (k), fuel velocity (Uj), pressure, preheating gas and air, and i (where i is the number of moles of oxygen combining with one mole of combustible gas).

When the value of i increases without changing the flow rate, an outward displacement of the flame front will be caused, then the flame will be lengthened. Meanwhile, the length of flame is inversely proportional to the coefficient of diffusion k, provided the other factors do not change. In our case, the value of i is 0.5 for H_2 and 2.0 for CH_4, the value of k is 0.71cm^2/s for H_2-air and 0.196cm^2/s for CH_4-air. Therefore, if under equal flame rate, the flame length of H_2 contained fuels should be much shorter than that of CH_4, and should get shorter and shorter with the increase of H_2 fraction.

Numerical simulations proved this rule clearly. Figure 4 showed the variety of maximum temperature's location along with the increase of volumetric fraction of H_2 predicted by CHEMKIN 4.1 with opposite flame model. In opposite flames, the location of the maximum temperature was exactly the location of flame front. The Y axis in figure 4 was the axial distance. As mentioned before, fuel was at 0cm and air was at 2cm distance. Therefore, this figure showed expressly that with the increase of H_2 fraction, the flame front moved toward the fuel side, hence, the flame length was shortened.

On the other hand, the vertical dimensions of a flame are directly proportional to the velocity of flow. Figure 5 took H_2 flame as an example to show the variety of flame length along with velocity (predicted by FLUENT simulation with Flamelet model). We could see clearly from the figure that with the increasing of fuel velocity, the flame length got longer.

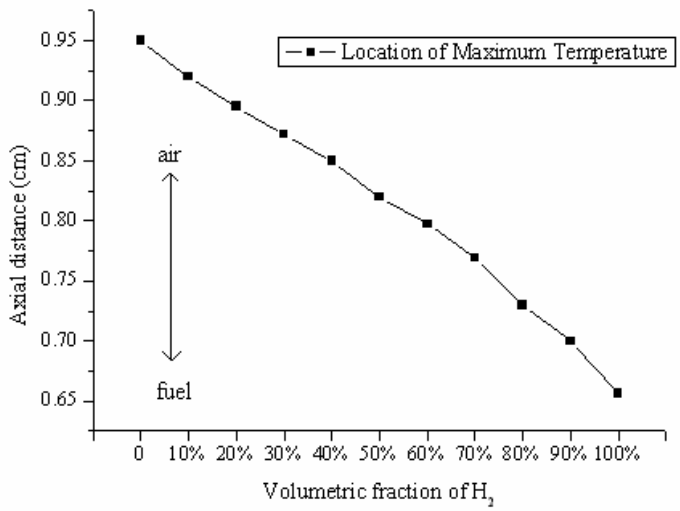

Fig.4 Location of Flame Front in Opposite Flames

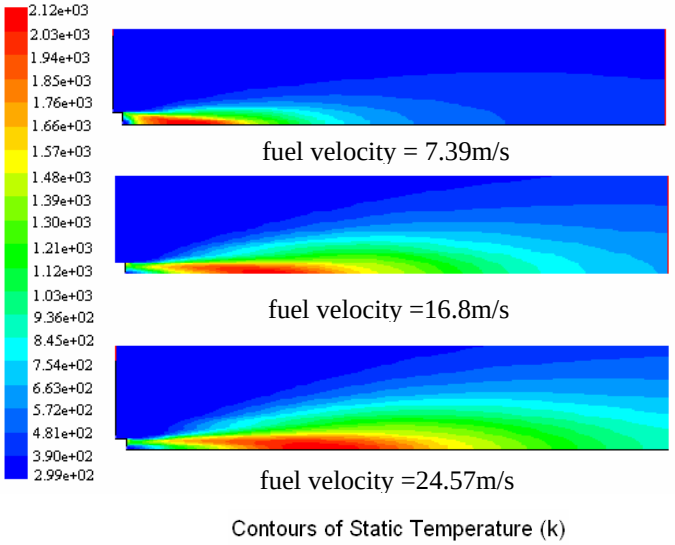

Fig.5 Flame Length under Different Velocity (H_2)

At last, to ravel the influence of tube dimension, CH_4, H_2, and 80%H_2+20%CH_4 was burned respectively through tube of ϕ6, ϕ11 and ϕ9, keeping equal power and equal velocity (7.39m/s). Photos of flames and results of simulations both showed that the flame length didn't change along with varying dimensions of tubes. That was consistent with the analysis of Burke and Schumann.

As analyzed above, when under equal flow rate, the flame length would get shorter with the increase of H_2 fraction due to its relative high value of k and low value of i. However, when compared under equal power, the fuel velocity would be increased due to the increase of flow rate along with H_2 fraction, which in turn extended the vertical flame dimension.

Thereby, the two contrary influences were both existed and might be counteracted partially with each other when increase the volumetric fraction of H_2 under equal power. That was the reason why flame length of fuels with various H_2 fractions had little difference in the experiments.

Flame Temperature

Flame temperature of CH_4, H_2, and $80\%H_2+20\%CH_4$ in ϕ6mm tube with velocity of 7.39m/s, 24.57m/s, and 16.8m/s respectively was measured in the experiment. 7 sections in different axial height (h = 1.7ϕ, 4.2ϕ, 10ϕ, 18.3ϕ, 33.3ϕ, 50ϕ, 75ϕ) were selected to be measured, per millimeter a point along radial direction. With such sufficient measuring points, a nephogram of temperature distribution could be contoured as figure 6. That was a very intuitionistic way for better understanding the differences of the three fuels on flame structure and temperature distribution. From figure 6, a recirculation zone could be seen clearly in the root of every flame. According to the experimental data, the maximum temperature of H_2 was 1733K, $80\%H_2+20\%CH_4$ was 1703K, and CH_4 was 1613K. All of the highest temperatures of the three fuels were presented at the recirculation zone of the flame. The difference was that the flame temperature of H_2 kept almost the same high value as in the recirculation zone at the height range of h=1.7ϕ to h=60ϕ, $80\%H_2+20\%CH_4$ kept its region of high temperature to about h=50ϕ, while CH_4 kept the region to h=40ϕ. An interesting phenomenon was found here, when comparing the temperature distribution nephogram with the photos of flames (fig.3). It seemed that the flame of CH_4 had the longest vertical dimension than the two others according to the photos, however, if temperature was concerned, the dimension of high temperature region was getting longer when increasing H_2 fraction in the fuel.

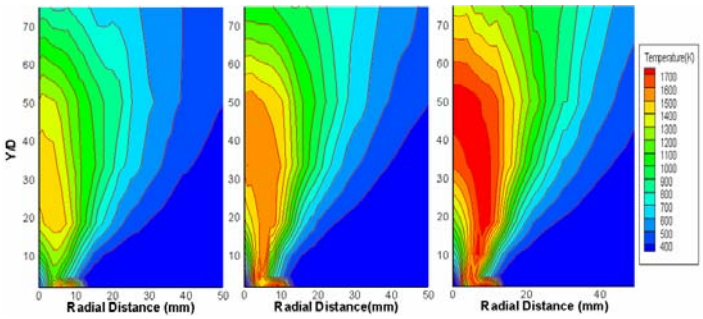

CH_4 $80\%H_2+20\%CH_4$ H_2

Fig. 6 Temperature Distribution by Experiment

FLUENT simulations were conducted to get flame information of other fuels. First of all, temperature data by simulations and by experiments were compared to find out the relatively best combustion model. Figure 7 took CH_4 flame as an example to show the results of the comparison. According to the figure, flame temperatures predicted by the Eddy-Dissipation and EDC model were much higher than the experiment, whereas temperatures predicted by Equilibrium model and Flamelet model were comparatively close to the experiment. That was also true for other fuels and other measuring height. Although all the models had a departure away from the experiment, the trend of temperature distribution predicted by Flamelet model was consistent enough with the practice.

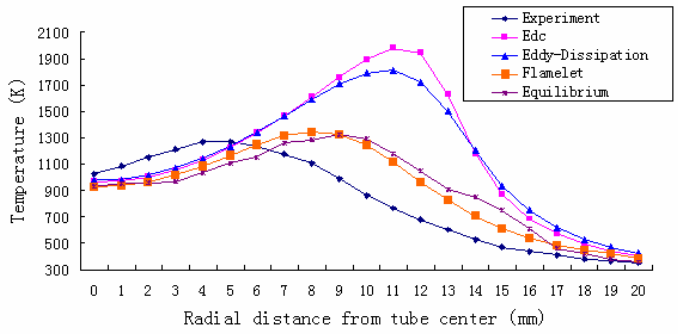

Fig.7 Temperature of CH_4 Flame (h=10ϕ)

Characteristics of Blowing out

Blowing out of the flames was observed through increasing the flow rate of air. For better understanding the changing tendency of flame structure along with the increasing of air flow rate, a scheme by I. ESQUIVA–DANO was quoted here [11]. In his paper, I. ESQUIVA–DANO described eight phases of flame changing with the decreasing of *Uj/Ue* (where *Uj* and *Ue* is the velocity of fuel and air respectively), showed in figure 8.

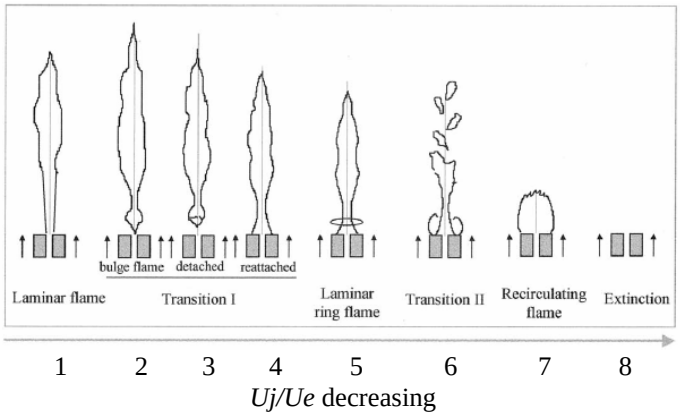

Fig.8 Characteristic regimes of non-premixed bluff-body stabilized flames [11].

During our experiments, H_2 and $80\%H_2+20\%CH_4$ presented the same tendency with figure 8. Figure 9 was photos of $80\%H_2+20\%CH_4$ flame, a quartz cylinder with inner diameter of 110mm and height of 200mm was fixed upon the burner. In photo (a), flame was in phase 2, that is, bulge flame. In photo (b), flame was lifted up, and reached phase 3, that is, detached flame. With the air flow rate increasing continuously, the flame reattached, passed the phase of 4~6, and reached phase 7 finally, showed as photo (c). Due to the limitation of experimental condition, the flame of $80\%H_2+20\%CH_4$ had

never been blew out. Flame of pure hydrogen showed same tendency with 80%H_2+20%CH_4. The photos of hydrogen flame were not showed here because of their faintness for observing.

(a) (b) (c)

Fig.9 Photos of 80%H_2+20%CH_4 Flames

(a) air flow rate = 7.2m^3/h (b) air flow rate = 9 m^3/h

(c) air flow rate = 60 m^3/h

What's worth to pay more attention is that the flame of pure CH_4 would be blew out so easily when the flow rate of air increased slightly. When the air flow rate reached 7.8m^3/h, the flame of CH_4 would be lifted up and then be blew out soon. It could never reach the 4-7 phases in the experiments.

Distribution of OH Concentration

Figure 10 and figure 11 was OH concentrations at the root of flame measured by PLIF. They are average images of 100 separate laser shots. The former was under equal tube diameter of Φ6, and the latter was under equal velocity of 7.39m/s. The range of measurement was pointed out on figure 3 (the red dashed panes). From figure 10, we could see that the combustion boundary of H_2 and 80%H_2+20%CH_4 was more clearly than CH_4, that is to say, at the root of the flame, combustion of H_2 was the most intensive one, 80%H_2+20%CH_4 took the second place, while CH_4 was the least. Figure 11 presented same tendency with figure 10. Meanwhile, in figure 11, distance between the two high OH concentration regions was larger along with the increase of tube diameter. This phenomenon showed clearly that the width of root flame would be extended with the increase of tube dimension.

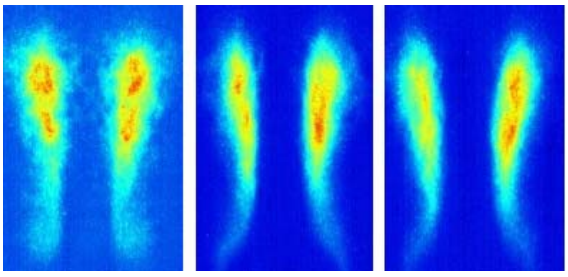

CH_4 (Φ6) 80%H_2+20%CH_4 (Φ6) H_2 (Φ6)

Fig. 10 OH Concentrations by PLIF (equal diameter)

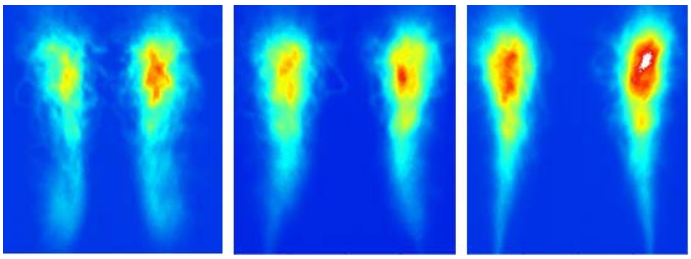

CH_4 (Φ6) 80%H_2+20%CH_4(Φ9) H_2(Φ11)

Fig. 11 OH Concentrations by PLIF (changing diameter)

NOx Emission

When measuring NOx emissions, the sampling probe entered into the chimney at the height of h=180Φ. Five points on the section were sampled, and NOx concentrations were gained by averaging values of the five points. Figure 12 showed the NOx concentrations on h=180Φ measured in experiments. According to the figure, NOx emission didn't show a linear relationship with the volumetric fraction of H_2 in fuels. There was an exponential uptrend. As was well known, NOx emissions were strongly related with the flame temperature. Therefore, the highest temperatures of fuels with various H_2 fractions predicted by FLUENT was showed in the same figure for visual antitheses. From the figure, a fairly well consistency could be found between the predicted temperature and the experimental NOx concentration. That was a good evidence again for proving the positive correlation between NOx emission and the flame temperature in combustion of hydrogen contained fuels.

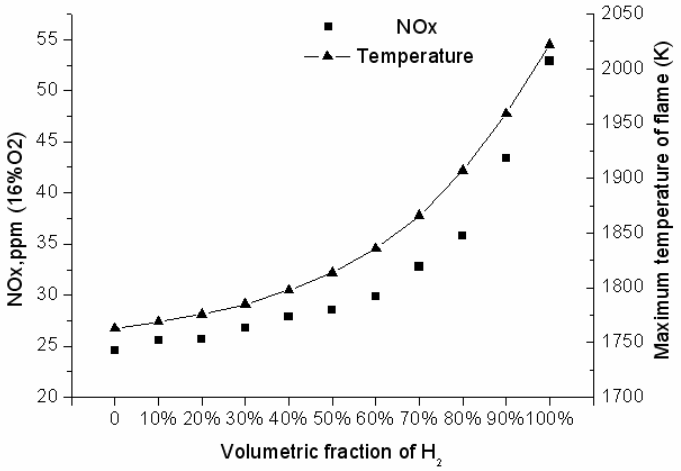

Fig. 12 NOx Concentration and Flame Temperature

On the other hand, a reduction of NOx concentration from 52.9ppm to 35.7ppm was gained when adding 20%CH_4 into the pure H_2 fuel, whereas with sequential increase of the CH_4 fraction to 100%, NOx emission reduced only from 35.7ppm to 24.6ppm. That is to say, the value of NOx reduction reached 17.2ppm through the first 20% addition of CH_4, but only

11.1ppm through the later 80% addition of CH_4. Thereby, if NOx emission was the only aspect to be considered, employment of $80\%H_2+20\%CH_4$ seemed to be a better choice for transition from pure CH_4 to pure H_2.

CONCLUSIONS

Detailed experimental measurements and numerical simulations were conducted to investigate the combustion characteristics of fuels with various volumetric H_2 fractions range from 0% to 100%. Comparison of H_2, CH_4, and $80\%H_2+20\%CH_4$ was the emphasis. According to the results showed by data of experiments and simulations, some conclusions could be drawn out through analysis.

In the extent of experiments, when under equal general power, the flame length of hydrogen contained fuels wasn't much shorter than methane, and didn't get shorter with the increase of H_2 fraction as expected. That was because the shortening tendency caused by the increase of H_2 fraction was counteracted partially by the increase of fuel velocity, results of which was the extending of flame length.

Maximum temperature of H_2 flame was 1733K, which was 30K higher than $80\%H_2+20\%CH_4$ and 120K higher than CH_4. All of the highest temperatures of the three fuels were presented at the recirculation zone of the flame. Although it seemed that the flame of CH_4 had the longest dimension than H_2 contained fuels when observed through photos, vertical dimension of the high temperature region of flames was getting longer when increasing H_2 fractions in the fuels. Curves of temperature distribution predicted by all the four combustion models in FLUENT investigated here had a departure away from the experimental data. Among the four models, Flamelet model was the one whose prediction was comparatively close to the experimental results.

Flame of H_2 and $80\%H_2+20\%CH_4$ had a much better stability than flame of CH_4, they could reach a so called recirculating flame phase and never been blew out in the extent of experiments. On the contrary, CH_4 flames were blew out easily soon after they were lifted up.

Distribution of OH concentration at the root of flames showed that the flame boundary of H_2 and $80\%H_2+20\%CH_4$ was more clearly than CH_4. That is to say, at the root of the flame, combustion of H_2 was the most intensive one, $80\%H_2+20\%CH_4$ took the second place, while CH_4 was the least.

NOx emissions didn't show a linear relationship with the volumetric fraction of H_2, but showed an exponential uptrend instead. It presented a fairly consistent tendency with the flame temperature, which proved again there was a strong relationship between flame temperature and NOx emissions in the combustion of hydrogen contained fuels.

If adding CH_4 into pure H_2, NOx concentration would have a 17.2ppm reduction with the first 20% accession, but only 11.1ppm with the later 80% accession. Hence, if NOx emission was the only aspect to be considered, employment of $80\%H_2+20\%CH_4$ seemed to be a competitive choice for transition from pure CH_4 to pure H_2.

ACKNOWLEDGMENTS

Thanks for the support by Natural Science Foundation of China (No. 50576098) and the National High Technology R&D Project of China (No. 2006AA05A104).

The author gratefully acknowledges the support of K.C. Wong Education Foundation, Hong Kong.

REFERENCES

1. Yuelong Yang, Wendong Tian, Yunhan Xiao, and Feng Wang, 2003, "Thermodynamic Analysis and Experimental Research on Direct Hydrogen Production From Carbonaceous Energy", *Journal of Engineering Thermophysics*, Vol 24, pp.744-746.
2. Chunzhen Qiao, Yunhan Xiao, 2005, "Comparison of Processes o f Hydrogen from Carbon and Analysis of Hydrogen from Carbon Direct", *Journal of Engineering Thermophysics*, Vol 26, pp.729-732.
3. Ahsan R. Choudhuri, S.R. Gollahalli, 2000, "Combustion Characteristics of Hydrogen-Hydrocarbon Hybrid Fuels", *Hydrogen Energy*, Vol 25, pp.451-462.
4. Ahsan R. Choudhuri, S. R. Gollahalli, 2003, "Characteristics of Hydrogen-Hydrocarbon Composite Fuel Turbulent Jet Flames", *Hydrogen Energy*, Vol 28, pp.445-454.
5. Mustafa Ilbas, Ilker Yilmaz, Yuksel Kaplan, 2005, "Investigations of Hydrogen and Hydrogen-Hydrocarbon Composite Fuel Combustion and NOx Emission Characteristics in a Model Combustor", *Hydrogen Energy*, Vol 30, pp.1139-1147.
6. F.Cozzi, A.Coghe, 2006, "Behavior of Hydrogen-Enriched Non-Premixed Swirled Natural Gas Flames", *Hydrogen Energy*, Vol 31, pp.669-677.
7. T.S.Cheng, C.-Y. Wu, C.-P. Chen, Y.-H.Li, et al, 2006, "Detailed Measurement and Assessment of Laminar Hydrogen Jet DIffusion Flames", *Combustion and Flame*, Vol 146, pp.168-282.
8. Cundy, V.A., Morse, J.S., and Senser D. W., 1986, "Constant-Tension Thermocouple Rake Suitable for Use in Flame Mod Combustion Studies", *The Review of Science Instruments, Vol.57*, pp.1209-1210
9. Sato, A., Hashiba, K, Hasatani, M., Sugiyama, S., and Kimura, J., A, 1975, "Correctional Calculation Method for Thermocouple Measurements of Temperatures in Flames", Combustion and FLame, Vol.24, pp.35-41.
10. S.P. Burke and T.E.W. Schumann, 1937, "Diffusion Flames", *Second Symposium on Combustion*, pp.1-11.
11. I. ESQUIVA–DANO, H. T. NGUYEN, and D. ESCUDIE*, 2001, "Influence of a Bluff-Body's Shape on the Stabilization Regime of Non-Premixed Flames", *Combustion and Flame*, Vol 127, pp. 2167-218